Photonics and lasing in liquid crystals

Lasers were invented some 40 years ago and are now used in a plethora of applications. Stable liquid crystals were discovered at about the same time, and are now the basis of a large display industry. Both technologies involve photonics, the former in the creation and use of light and the latter in the control and manipulation of light. However, it is only recently that these two mature technologies have been combined to form liquid-crystal lasers, heralding a new era for these photonic materials and the potential for novel applications. We summarize the characteristics of liquid crystals that lead to laser devices, the wide diversity of possible laser systems, and the properties of the light produced.

Alison D. Ford, Stephen M. Morris, and Harry J. Coles*

Centre of Molecular Materials for Photonics and Electronics, Electrical Engineering Division, Cambridge University, Engineering Department, 9 J. J. Thomson Avenue, Cambridge CB3 0FA, UK

**E-mail: hjc37@cam.ac.uk*

Band gaps in materials have long been recognized as important for waves propagating in regular periodic structures, e.g. electron waves in semiconductor materials, sound waves in phononic crystals, and more recently electromagnetic waves in photonic crystals. Band gaps arise essentially from interference effects between waves as they propagate through the medium in question. This article is concerned with photonic band gap (PBG) structures produced in liquid crystals (LCs) where phases with a regular, periodic dielectric structure may be used to generate coherent laser light or amorphous phases may be used to generate random lasing. The soft matter nature of these materials and their response to external stimuli leads to readily tunable laser light that may be generated in the near ultraviolet through the visible spectrum to the near infrared. The broad wavelength tuning range of LC lasers, coupled with their microscopic size, narrow linewidths (< 0.1 nm), and high optical efficiencies as compared with more conventional solid-state lasers, will open up new applications in areas such as labs-on-a-chip, medical diagnostics, dermatology, holography, etc.

This article focuses on the material properties of the LC phases that give rise to PBGs, before proceeding to discuss LC band-edge lasers in the context of generic laser properties such as threshold behavior, coherent emission, and their dependence upon the nature of the LC host. As is well known from the display industry, the optical properties of LC displays (LCDs) are readily altered by external factors such as electric fields, temperature changes, or mechanical deformations. The

ISSN:1369 7021 © Elsevier Ltd 2006

implications of such responses for tunable laser emission are discussed. Finally, we consider alternative lasers, such as the defect-mode and random laser, as well as potential applications for these highly tunable microlasers.

LCs as PBG materials

A wide range of LC phases exist with varying degrees of orientational and/or positional order. These self-organizing, soft-matter materials may be composed of molecules that are chiral or nonchiral. Generally, chiral LCs self organize to give a macroscopic helical phase (denoted by an asterix) with a structure that exhibits a PBG, provided that the wavelength of incident light is of the helical periodicity. Such structures exhibit the optical properties of a solid while simultaneously possessing fluidity.

In general, the molecules in LC media favor a certain orientation as a result of intermolecular forces. On average, the long axis of the molecules aligns parallel to a common direction termed the director ***n***. The simplest LC phase to form a photonic band structure is the chiral nematic (N*) phase, where the director ***n*** precesses orthogonally and continuously around a single direction, giving a helical structure (Fig. 1). One full rotation of the director around the helix axis describes the pitch of the helix, although the structure repeats itself over a distance equal to half the pitch (the period) because of the inversion symmetry of the director[1]: ***n*** = -***n***. Since the periodicity exists in only one direction (i.e. along the helix axis), the PBG also only exists in the same unique direction.

Linearly polarized light that is incident parallel to the helix axis of the chiral nematic LC can be considered as two circularly polarized waves with opposite handedness. A PBG occurs for the circular polarized mode that matches the rotation sense of the helix when the wavelength is of the order of the pitch. For the other circular polarized mode with opposite sense handedness, the light is transmitted. Measurement of the transmission (or reflection) spectrum defines the PBG, where the decrease (or increase) in light intensity indicates the range of wavelengths forbidden to propagate.

By considering the chiral nematic LC as a series of anisotropic rotating layers, de Vries[2] showed that the bandwidth of the reflection band $\Delta\lambda$ is proportional to both the helix pitch P and the birefringence Δn, so that $\Delta\lambda = \Delta n.P$, where $\Delta n = n_{//} - n_{\perp}$ and the subscripts refer to the parallel and perpendicular components of the refractive index relative to the local director, respectively.

The chiral smectic C* LC phase, like the chiral nematic LC, also exhibits a helical structure and consequently a one-dimensional PBG. The molecular arrangement in the chiral smectic C* phase is illustrated in Fig. 2. While the director of a chiral nematic LC precesses normally around the helix axis, in a chiral smectic C phase, the molecules tilt at an angle to the helix axis. The LC molecules form soft layer planes with an alternating high and low density of molecular cores separated by regions of highly mobile hydrocarbon chains.

In contrast, a blue phase (BP) is an intermediate phase observed on cooling the LC from the isotropic phase (that has random molecular orientations) to the chiral nematic phase[1]. There are three different BPs named BPI, BPII, and BPIII, where BPIII is often termed the fog or amorphous phase. BPI and BPII adopt an elegant, double-twist structure where macroscopic packing constraints of the double-twist helices lead to a regular array of defect lines with a cubic structure[3]. These BPs are best described as fluid lattices of defects. The lattice spacing between the defects is of the same order as visible light wavelengths and occur

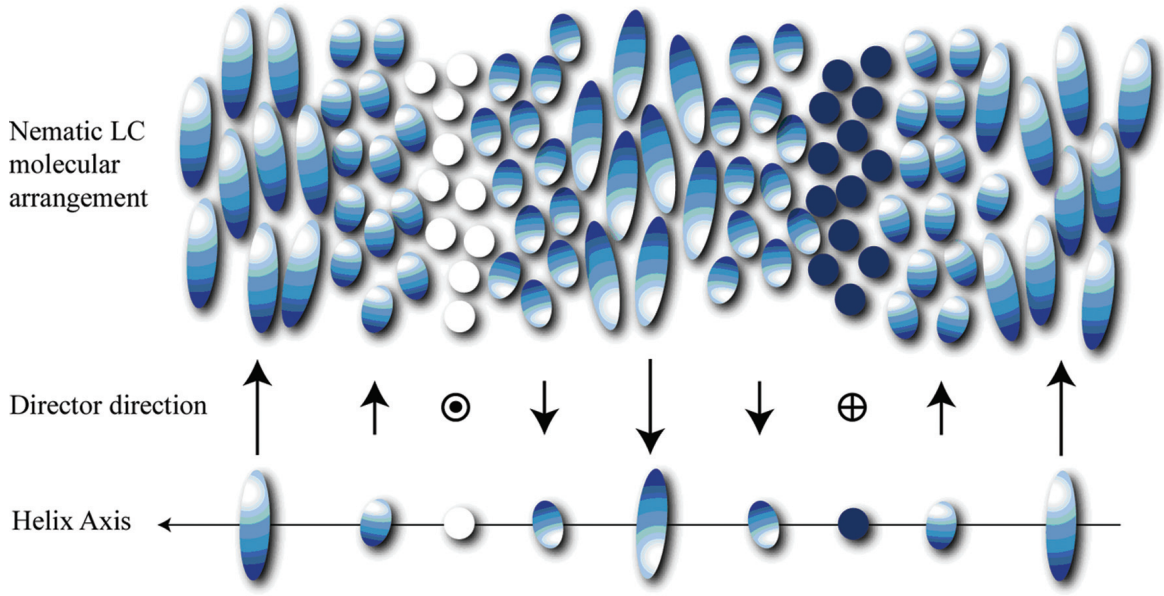

*Fig. 1 Schematic of the molecular configuration of one full pitch of a chiral nematic LC showing the director direction **n** and the helix axis.*

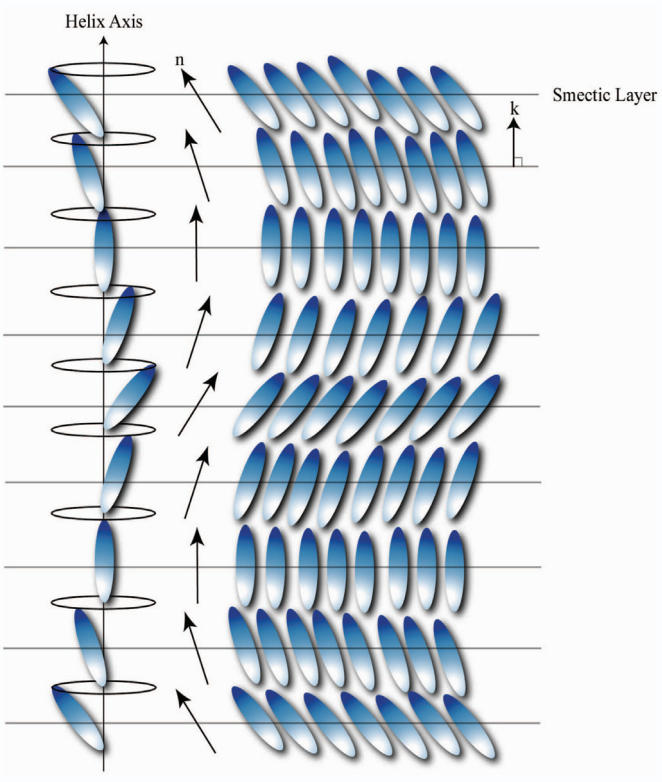

*Fig. 2 Molecular configuration of one pitch of the chiral smectic C phase showing the layer planes, the layer normal **k**, the director **n**, and the helix axis.*

in three dimensions. These give rise to Bragg reflections that consequently lead to a three-dimensional PBG being observed.

LC band-edge lasers

A typical LC laser consists of an LC host and a fluorescent laser dye, where the LC host provides the feedback and the laser dye provides the gain. The original concept of lasing in liquid crystals was put forward by Goldberg and Schnur[4] in a patent in 1973. It described a 'tunable internal-feedback liquid crystal dye laser' involving a liquid lasing medium with internal distributed feedback by virtue of the chiral nematic LC structure. This patent recognized the work of Kogelnik and Shank[5], who examined the distributed feedback laser in the context of the coupled mode theory. However, it took 25 years before LC lasing was experimentally demonstrated by Kopp *et al.*[6] in 1998.

During the years between the prediction and demonstration of lasing in LCs, considerable research was conducted into the optical properties of materials exhibiting a PBG. In 1981, Il'chishin and coworkers[7] demonstrated the modification of fluorescent emission in the presence of a PBG. In contrast, Yablonovitch[8] examined the optical properties of the PBG itself, and suggested that photon suppression would occur within the PBG. John[9] also showed that photon localization and enhancement would occur at the photonic band edges (PBEs) and Dowling and colleagues[10] reported that, with the inclusion of a fluorescent emitter, spontaneous emission would be suppressed within a PBG and enhanced at the band edges where there is a sharp increase in the density of photon states (DoS). It is here at the PBEs that lasing occurs on the inclusion of such a gain medium, as first reported by Kopp *et al.*[6].

A theoretical treatment by de Vries[2] of the interaction of light with a chiral nematic LC showed that the wavevector ***k*** is imaginary in the chiral nematic reflection spectrum, thus giving rise to an evanescent wave. Consequently, the DoS and spontaneous emission are zero. In contrast, the DoS diverges at the edges of the reflection spectrum, decreasing the group velocity and increasing the photon dwell time. Thus, the stimulated emission rate is large at the edges. As a result, two possible laser channels exist in an LC laser: one at each band edge. The wide spacing of these two modes because of the presence of the PBG restricts mode hoping, which is a common disadvantage with more conventional lasers, such as the Fabry-Perot laser[11]. Schmidtke and Stille[12] showed that the magnitudes of the peaks at the band edges are equal, indicating that both edges are potentially suitable for lasing.

Fig. 3a shows LC lasing at the band edge, where the black curve shows the transmission spectrum and the decrease in the transmission between 524 nm and 614 nm indicates the PBG. The red line shows the LC laser emission that corresponds to the lower energy band edge of the PBG. Fig. 3b shows the actual laser line shape on a magnified

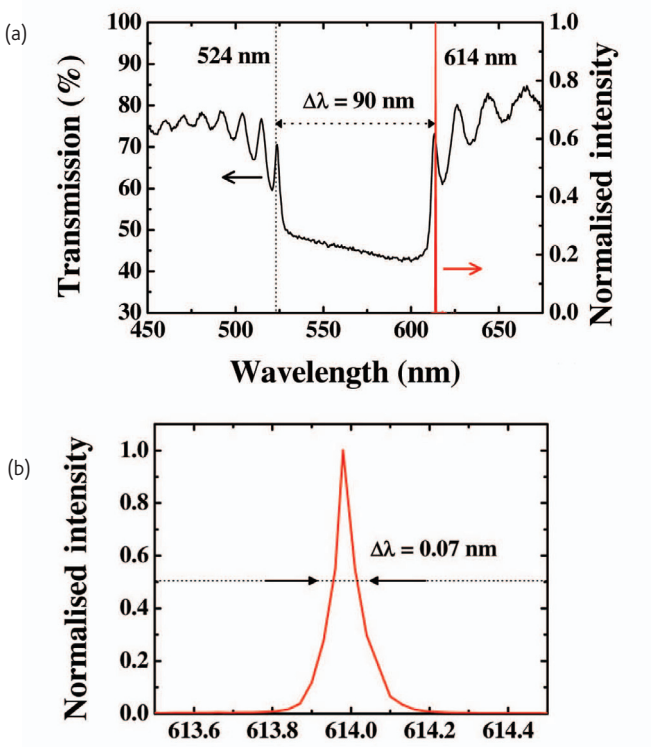

*Fig. 3 (a) The N*LC transmission spectrum (primary axis) and the LC laser emission spectrum (secondary axis). (b) LC laser emission spectrum measured using a spectrometer with a spectral resolution of 0.04 nm.*

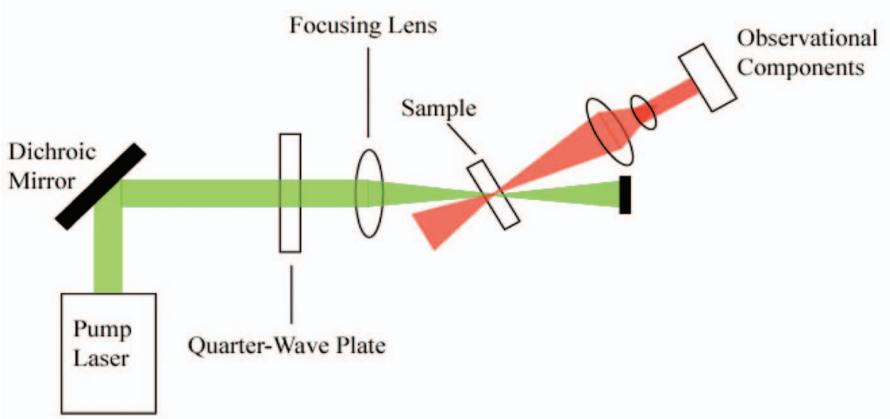

Fig. 4 Schematic of an experimental setup for studying LC lasers.

wavelength scale, giving a linewidth of 0.07 nm. Chirality in an LC can be naturally forming in the bulk material itself or, for an achiral host, can be induced on addition of a high-twisting-power chiral additive. The latter approach allows the macroscopic optical properties of the LC as desired, while the chiral additive allows the position of the band edge to be selected for a specific wavelength output.

Fig. 4 shows a typical experimental setup where an LC laser sample is optically pumped with a pulsed laser. The wavelength of the pump laser must coincide with the absorption of the laser dye. A typical combination is to pump the laser dye 4-(dicyanomethylene)-2-methyl-6-(4-dimethylaminostryl)-4*H*-pyran optically with a Nd:YAG laser frequency doubled to 532 nm with pulse widths of either nanoseconds or picoseconds. The penetration depth of the excitation beam in the LC laser sample is maximized by converting the linearly polarized pump laser beam into circularly polarized light through the use of a quarter-wave plate. The LC laser emission properties can be measured using a range of components, e.g. a spectrometer, energy meter, beam profiler, etc. Furthermore, while a typical LC laser consists of an LC host and fluorescent laser dye, it is not always essential to include the fluorescent dye. The natural fluorescence of the LC host can provide sufficient gain to achieve lasing at short wavelengths[13].

LC band-edge lasers exhibit the same characteristics as a typical laser[6,14,15], i.e. threshold behavior (as in Fig. 5, where the discontinuity in the slope represents the threshold), narrow linewidths (~0.07 nm, e.g. Fig. 3b), near-Gaussian emission profiles (Fig. 6), and coherent, directional emission (Fig. 7).

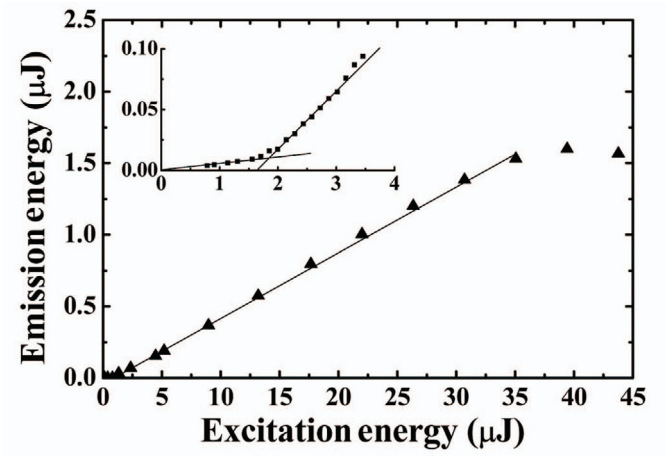

Fig. 5 Emission energy of an LC laser as a function of excitation energy, using 6 ns pump pulses operated at 1 Hz. The inset magnifies the threshold region.

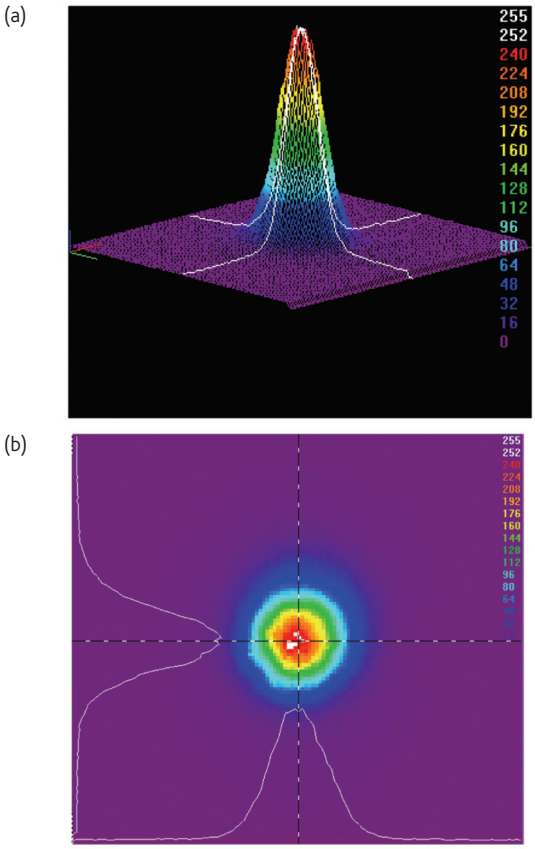

*Fig. 6 Emission profile of an N*LC laser in (a) three and (b) two dimensions. The beam waist is ~ 50 μm and the images were taken ~ 5 cm away from the LC laser source.*

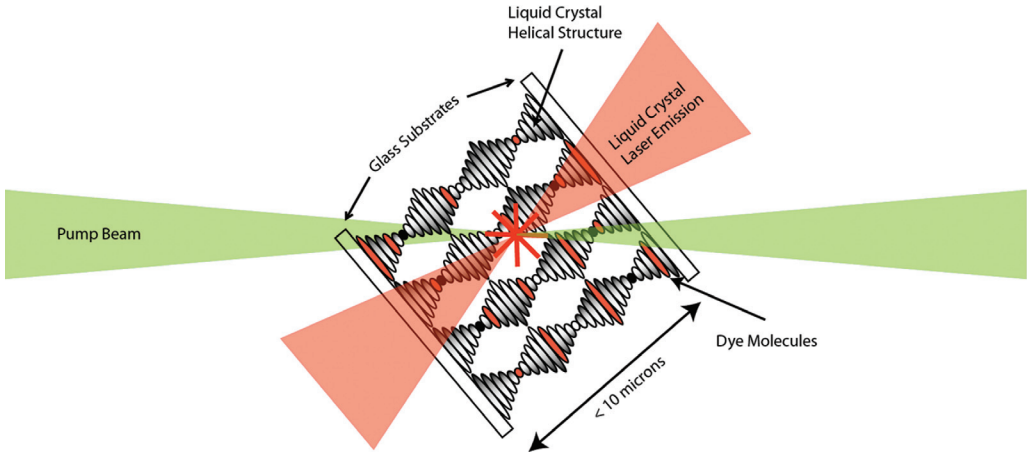

Fig. 7 Illustration of LC laser emission parallel to the helix axis of the LC in both forward and backward directions. The pump beam is incident at an angle to the helix axis.

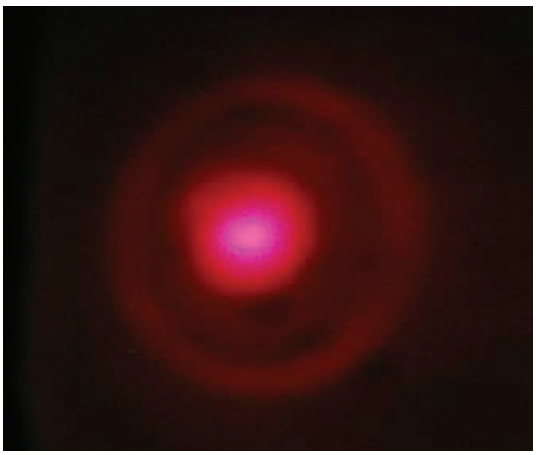

Fig. 8 Photograph of the far-field interference pattern from an LC laser.

LC laser emission always occurs in a direction parallel to the helix axis irrespective of the angle of incidence of the pump beam. This is illustrated in Fig. 7, where the pump beam intersects the LC laser sample at an angle, while the LC laser emission occurs in a direction parallel to the LC helix axis. Interference rings are observed in the far-field emission (~50 cm from the LC laser source)[14,15], as shown in Fig. 8. Because of the symmetry of the helical LC structure, laser emission occurs equally in both the forward and the backward directions.

Material properties of the LC host

The macroscopic physical properties of the LC host strongly affect the emission characteristics of the LC laser. The LC laser is analogous to a distributed feedback (DFB) laser for which the laser threshold can be described as a function of the birefringence. It has been shown that the macroscopic LC birefringence greatly influences the LC laser threshold. An increase in the birefringence gives rise to a decrease in the laser threshold[16,17] because of the direct relationship between the birefringence and the DoS at the band edge[18]. The LC birefringence is intrinsically a function of the orientational order parameter[19] and, consequently, a higher degree of order within the system gives rise to lower threshold energies and high slope efficiencies, where the latter is defined by the ratio of the increase in emission energy to the increase in excitation energy.

A measure of the dye emission efficiency can be obtained from the order parameter of the transition dipole moment of the dye[20,21]. Perfect alignment of the dye molecules with the LC molecules is preferable if LC laser emission occurs at the long-wavelength PBE, whereas normal alignment of the dye with the LC molecules is better for laser emission at the short-wavelength PBE.

In addition, an LC with a large bulk viscosity restricts the thermal and rotational motion of the dye molecules, thus reducing nonradiative emissions within the system[22] and reducing the laser threshold energy. Consequently, the molecular design of the LC host and its macroscopic properties are of significant importance for optimized laser performance.

The chiral smectic C* and glass phases may exhibit higher degrees of orientational order and higher viscosities than the chiral nematic LC phase[1]. LC lasers using these phases have lower laser thresholds than chiral nematic LC lasers[22-24]. The implication is that an increase in order and viscosity reduces the laser threshold because of the reduction in nonradiative losses.

Threshold energies lower than those observed for a chiral nematic LC laser are also observed when BPI and BPII provide the host[17,25,26]. In these cases, the three-dimensional PBG provides confinement of the spontaneous emission within the system, thus restricting losses and reducing the laser threshold. While the one-dimensional PBG of chiral nematic and chiral smectic C* phases gives rise to emission along the helix axis, the three-dimensional PBG of a blue phase can result in laser emission in three different directions[25].

Tunability

LC media characteristically exhibit a strong response to external influences. The behavior of the LC and, hence, the PBG is of significant

importance because the band edges define the wavelengths of the laser output. The application of external influences, such as a variation in the operating temperature, an applied electric field, or a mechanical stress, allows direct control and modification of the helix pitch, which can be used to tune the LC laser wavelength.

The temperature dependence of PBEs is determined by the temperature dependence of the refractive indices and the pitch. A thermochromic chiral nematic LC shows a rapid divergence in pitch on cooling as the material starts to transform into a higher ordered phase. This is exactly the same mechanism as used in LC thermometers, fever sensors, etc. This mechanism may be used to tune the LC laser cavity.

Typically, an LC laser uses a polyimide alignment layer on the inner surfaces of the glass substrates of the cell. The anchoring produced by the alignment layer causes the pitch to vary discontinuously[27-29] while the refractive indices vary continuously with temperature[1]. Both mechanisms can be used to tune the LC laser wavelength[30,31]. Alternatively, a variation in the pitch across the cell can be induced by introducing a temperature gradient, through which a translation of the sample relative to the pump beam results in LC laser wavelength tuning[32]. Similarly, a pitch gradient can also be introduced across the cell by varying the concentration of the chiral dopant used to induce the helix[33].

The dielectric anisotropy of the LC media gives rise to molecular reorientation in the presence of an electric field, provided that the field is larger than a certain threshold value (the Fréedericksz threshold). The application of an electric field to an LC laser deforms the helix in a fashion that depends upon the direction of the field in relation to the helix axis[34-38] and therefore tunes the emission wavelength.

A range of additional tuning mechanisms also exists. Finklemann *et al.*[39] have demonstrated LC laser wavelength tuning through modification of the helix in a cholesteric elastomer under an external mechanical stress. A number of reports[40-43] have used ultraviolet illumination to alter the structure of one or more of the LC components. Shibaev and colleagues[44] have tuned the laser emission wavelength of cholesteric polymers that are sensitive to pH changes.

Despite the wide variety of tuning mechanisms, the range of wavelengths available for tuning is generally restricted by the wavelength range of the fluorescence spectrum of the doped dye. However, this tunability range can be increased by incorporating several resonant dyes into the system. A combination of dyes that decouples the excitation and emission processes through the Forster transfer process[45,46] provides a gain spectrum ranging from the ultraviolet through the visible to the infrared[47].

Influence of experimental design conditions

In addition to the material properties of the LC host influencing LC laser emission characteristics, the experimental optical pumping conditions also have a significant effect. Morris *et al.*[48] found a significant decrease in the LC laser emission energies when operated at pump repetition rates much greater than a few hertz. This is thought to be the result of director reorientation arising from the intense optical field of the pump laser. Cao and coworkers[16] report that decreasing the pump pulse width from nanoseconds to picoseconds gives rise to a decrease in the LC laser threshold. The magnitude of the decrease is influenced by the concentration of the laser dye dopant, and was discussed in the context of excimer formation within the dye.

Alternative LC lasers

In addition to the LC band-edge laser, three other types of laser that use LCs have been demonstrated: the random laser, the defect-mode laser, and the photonic crystal infiltrated with an LC laser.

The random laser[49,50] relies on the multiple scattering of a photon within a medium giving rise to strong amplification, provided that there is sufficient gain present. Random lasers are usually achieved by doping additional scattering particles, such as sintered glass, into a high-gain medium, such as a laser dye. A number of materials have been used to generate random lasers. These include doping a laser dye with spherical dielectric scatterers[51], nanoclusters of ZnO[52], or dye-infiltrated opals[53]. The use of nematic LCs as random lasers has been shown[54], where sintered glass was added to the LC/laser dye solution to enhance the scattering. The thermal properties of the LC were then used to switch the laser 'on' and 'off'. Alternative LC configurations have also been shown to behave as random lasers. For instance, the application of an electric field to a dye-doped smectic A phase[55] induces a highly turbid texture, where the electric field enables direct control of the number of scattering centers within the sample and thus the emission intensity. Similarly, the application of an electric field to a polymer-dispersed LC (PDLC) can induce a highly turbid texture from which random lasing can also be achieved[56]. Adding dyes to a PDLC laser also results in marked linewidth narrowing[57].

Defect-mode lasing is observed when a defect mode is introduced into the chiral structure, giving rise to an additional resonant mode inside the PBG[58]. The introduction of the defect disrupts the periodicity of the dielectric structure resulting in a 'leaky' mode at the centre of the band gap where lasing occurs. This can be achieved by either replacing a thin layer of the cholesteric LC with an isotropic liquid or by introducing a phase jump into the helix structure[59]. A recent report[60] discusses the use of partially reflecting glass slides of random thicknesses with rhodamine 6G dyed spacer layers. Milner and Genack[60] pumped the medium at a resonant mode that enhances the penetration of the pump beam into the sample. This reduces the absorption losses, which is necessary to reduce the LC laser threshold.

In principle, a specific resonant wavelength of an optical cavity can be tuned by adjusting the cavity's refractive index and therefore the effective optical path length. Using LCs within a photonic crystal cavity provides a method for varying the refractive index through a simple manipulation, such as applying an electric field. It has been shown that, after introducing an LC into a photonic crystal cavity, the effective

refractive index can be varied on application of an electric field to tune the resonance conditions[61].

Applications and the future

The LC laser appears to have a great future. Their small size, with length scales of the order of tens to hundreds of microns, and high versatility enable them to operate as light sources that are tunable from ultraviolet wavelengths, through the visible range, to infrared wavelengths. The material properties of the LC host can be manipulated not only to vary the laser threshold energy[16] and slope efficiency[17] but also to provide alternative laser device designs. For example, polymerization of an LC laser gives rise to a flexible laser device[62]. The performance of these lasers is continually improving. Recent reports have achieved optical slope efficiencies of between 20% and 30% by improving the dye/LC host combination[17] or the LC host molecular structure[63]. Such efficiencies are comparable to more conventional solid-state microlaser sources when operated in similar wavelength regions[64].

Potential applications for this technology include labs-on-a-chip, spectroscopy, displays, and a wide variety of medical applications. In addition, recent work[65] has demonstrated the use of an LC laser as an electrotunable optical diode. Currently, however, it is necessary to optically pump these systems with pulsed lasers, which restricts their range of potential applications. To achieve continuous wave operation of LC lasers, it will be necessary to reduce the threshold through material design taking into account the LC properties discussed above, minimize internal cavity losses resulting from absorption, and optimize the LC cavity design. A significant reduction in the threshold would increase the number of potential pumping mechanisms that might be available for use, such as a light-emitting diode or white light source. This will, in turn, increase the potential applications for these highly versatile, soft-matter microlasers. mt

REFERENCES

1. See, for example, Collings, P. J., *Liquid Crystals: Nature's Delicate Phase of Matter*, Adam Hilger, Bristol, UK (1990)
2. de Vries, H., *Acta Crystallogr.* (1951) **4**, 219
3. Kitzerow, H., and Bahr, C., (eds.), *Chirality in Liquid Crystals*, Springer, New York, (2001), Chapter 9
4. Goldberg, L. S., and Schnur, J. M., US Patent 3,771,065, Nov 6, 1973
5. Kogelnik, H., and Shank, C. V., *J. Appl. Phys.* (1972) **43**, 2327
6. Kopp, V. I., *et al., Opt. Lett.* (1998) **23**, 1707
7. Il'chishin, *et al., JETP Lett.* (1980) **32**, 24
8. Yablonovitch, E., *Phys. Rev. Lett.* (1987) **58**, 2059
9. John, S., *Phys. Rev. Lett.* (1987) **58**, 2486
10. Dowling, J. P., *et al., J. Appl. Phys.* (1994) **75**, 1896
11. See, for example, Svelto, O., *Principles of Lasers*, 4th edition, Plenum Press, New York, (1998)
12. Schmidtke, J., and Stille, W., *Eur. Phys. J. B* (2003) **31**, 179
13. Munoz, A., *et al., Opt. Lett.* (2001) **26**, 804
14. Kopp, V. I.. *et al., Phys. Rev. Lett.* (2001) **86**, 1753
15. Kopp, V. I., *et al., Prog. Quantum Electron.* (2003) **27**, 369
16. Cao, W., *et al., Mol. Cryst. Liq. Cryst.* (2005) **429**, 101
17. Morris, S. M., *et al., J. Soc. info. Display* (2006) **14**, 565
18. Woon, K. L., *et al., Phys. Rev. E* (2005) **71**, 041706
19. Morris, S. M., *et al., J. Appl. Phys.* (2005) **97**, 023103
20. Araoka, F., *et al., J. Appl. Phys.* (2003) **94**, 279
21. Shin, K.-C., *et al., Jpn. J. Appl. Phys.* (2004) **43**, 631
22. Shibaev, P., *et al., Liq. Cryst.* (2003) **30**, 1391
23. Ozaki, M., *et al., Adv. Mater.* (2002) **14**, 306
24. Ford, A. D., *et al., Proc. SPIE* (2004) **5289**, 213
25. Cao, W., *et al., Nat. Mater.* (2002) **1**, 111
26. Yokoyama, S., *et al., Adv. Mater.* (2006) **18**, 48
27. Zink, H., and Belyakov, V. A., *J. Exp. Theor. Phys.* (1997) **85**, 285
28. Belyakov, V. A., and Kats, E. I., *J. Exp. Theor. Phys.* (2000) **91**, 488
29. Belyakov, V. A., *et al., J. Exp. Theor. Phys.* (2003) **96**, 915
30. Funamoto, K., *et al., Jpn. J. Appl. Phys.* (2003) **42**, L1523
31. Moreira, M. F., *et al., Appl. Phys. Lett.* (2004) **85**, 2691
32. Huang, Y., *et al., Appl. Phys. Lett.* (2006) **88**, 011107
33. Chanishvili, A., *et al., Adv. Mater.* (2004) **16**, 791
34. Kasano, M., *et al., Appl. Phys. Lett.* (2003) **82**, 4026
35. Ozaki, M., *et al., Adv. Mater.* (2003) **15**, 974
36. Furumi, S., *et al., Appl. Phys. Lett.* (2003) **82**, 16
37. Yu, H., *et al., Opt. Express* (2005) **13**, 7243
38. Morris, S. M., *et al., Proc. SPIE* (2005) **5741**, 118
39. Finkelmann, H., *et al., Adv. Mater.* (2001) **13**, 1069
40. Furumi, S., *et al., Appl. Phys. Lett.* (2004) **84**, 2491
41. Fuh, A., *et al., Opt. Express* (2004) **12**, 1857
42. Chanishvili, A., *et al., Appl. Phys. Lett.* (2003) **83**, 5353
43. Shibaev, P., *et al., Opt. Express* (2005) **13**, 2358
44. Shibaev, P. V., *et al., Chem. Mater.* (2004) **16**, 1397
45. Alvarez, E., et al., *Mol. Cryst. Liq. Cryst.* (2001) **369**, 75
46. Chambers, M., et al., *Adv. Funct. Mater.* (2002) **12**, 808
47. Chanishvili, A., *et al., Appl. Phys. Lett.* (2005) **86**, 051107
48. Morris, S. M., *et al., J. Opt. A: Pure Appl. Opt.* (2005) **7**, 215
49. Cao, H., *IEEE J. Sel. Top. Quantum Electron.* (2003) **9**, 111
50. Ling, Y., et al., *Phys. Rev. A* (2001) **64**, 063808
51. Lawandy, N. M., *et al., Nature* (1994) **368**, 436
52. Cao, H., *et al., Phys. Rev. Lett.* (1999) **82**, 2278
53. Frolov, S. V., *et al., Opt. Commun.* (1999) **162**, 241
54. Wiersma, D. S., and Cavalieri, S., *Nature* (2001) **414**, 708
55. Morris, S. M., *et al., Appl. Phys. Lett.* (2005) **86**, 141103
56. Gottardo, S., *et al., Phys. Rev. Lett.* (2004) **93**, 263901
57. Harada, H., et al., *Jpn. J. Appl. Phys.* (2005) **44**, L915
58. Kopp, V. I., and Genack, A. Z., *Phys. Rev. Lett.* (2002) **89**, 033901
59. Schmidtke, J., *et al., Phys. Rev. Lett.* (2003) **90**, 083902
60. Milner, V., and Genack, A. Z., *Phys. Rev. Lett.* (2005) **94**, 073901
61. See, for example, Maune, B., *et al., Appl. Phys. Lett.* (2004) **85**, 360
62. Matsui, T., *et al., Appl. Phys. Lett.* (2002) **81**, 3741
63. Morris, S., *et al.*, unpublished results
64. Hastie, J., *et al., Opt. Express* (2005) **13**, 77
65. Hwang, J., *et al., Nat. Mater.* (2005) **4**, 383